Centro Euro-Mediterraneo sui Cambiamenti Climatici

The new CMCC Operational Seasonal Prediction System

Technical Notes
September 2020
Issue TN0288

CMCC DIVISION
Climate Simulations and Precitions

By ***Silvio Gualdi***
Fondazione CMCC Centro Euro-Mediterraneo sui Cambiamenti Climatici
silvio.gualdi@cmcc.it

Andrea Borrelli
Fondazione CMCC
andrea.borrelli@cmcc.it

Antonio Cantelli
Fondazione CMCC
antonio.cantelli@cmcc.it

Guido Davoli
Fondazione CMCC
Università Ca' Foscari Venezia
guido.davoli@unive.it

Maria del Mar Chaves Montero
Fondazione CMCC
mariadm.chaves@cmcc.it

Simona Masina
Fondazione CMCC
simona.masina@cmcc.it

Antonio Navarra
Fondazione CMCC
antonio.navarra@cmcc.it

Antonella Sanna
Fondazione CMCC
antonella.sannai@cmcc.it

Stefano Tibaldi
Fondazione CMCC
stefano.tibaldii@cmcc.it

C3S Service Contract 2018/C3S_330_CMCC.

SUMMARY The purpose of this report is to provide information on the new version of the operational CMCC SPS3.5 Seasonal Prediction System/Model(s) version which will replace in operations the former version SPS3 starting from the operational forecast of October 1st, 2020. The new version differs from the previous one essentially only for the horizontal resolution of the atmospheric model component (CAM 5.3), plus a number of comparatively minor details which will be mentioned below. All hindcasts previously available (1993-2016) have also been rerun, for the same dates, at the new, higher, atmospheric model resolution, all other system characteristics having remained essentially the same.

Keywords Numerical Seasonal Forecasts, Ensemble Climate Predictions, Numerical Models, Interannual Climate Variability.

DOI: https://doi.org/10.25424/CMCC/SPS3.5

1. INTRODUCTION

The purpose of this report is to provide information on the new version of the operational CMCC SPS3.5 Seasonal Prediction System/Model(s) version which will replace in operations the former version SPS3 starting from the operational forecast of October 1st, 2020. The new version differs from the previous one essentially only for the horizontal resolution of the atmospheric model component (CAM 5.3), plus a number of comparatively minor details which will be mentioned below. All hindcasts previously available (1993-2016) have also been rerun, for the same dates, at the new, higher, atmospheric model resolution, all other system characteristics having remained essentially the same.

2. THE CMCC SPS3.5 OPERATIONAL SEASONAL PREDICTION SYSTEM

2.1 THE OPERATIONAL PREDICTION SYSTEM

The acronym and full name of the System is CMCC-SPS3.5, i.e. Euro-Mediterranean Center for Climate Change - Seasonal Prediction System, Version 3.5. The System is based on a coupled Ocean-Atmosphere Global Climate Model, complemented by a number of additional modules. The System is operated monthly in Ensemble seasonal mode (6-month predictions) and is completed by a database of monthly ensemble hindcasts covering the period 1993-2016 which can be used to evaluate the performance of the System and to apply bias removal techniques from operational forecasts. The first operational seasonal forecast run produced for C3S with CMCC-SPS3, and contained in the CDS, was initiated from April 1st, 2018, 00:00 UTC and monthly, from the first day of every month, up to September 1st, 2020. All further monthly seasonal forecasts (all with a forecast horizon of six months) from January 1st, 2017 until March 1st, 2018 are also available as POPs, Pre-Operational Predictions. From October 1st, 2020, CMCC-SPS3 has been replaced in operations by CMCC-SPS3.5. All these forecasts and hindcasts constitute, together, a continuous database of monthly ensemble seasonal (6-month) forecasts from January 1st, 1993 up to the present date.

System Name:	CMCC-SPS3.5
Forecast frequency:	Monthly.
Forecast time range:	Six-month.
Forecast nominal start date:	1st of the month.
Forecast ensemble size:	50 members in operational and pre-operational prediction mode, 40 members in hindcast mode.
Operational Forecast time-span:	October 2020 – Now.
Hindcast time-span:	January 1993 - December 2016.

Figure 1: General scheme of the CMCC-SPS3.5 fully coupled Seasonal Prediction System

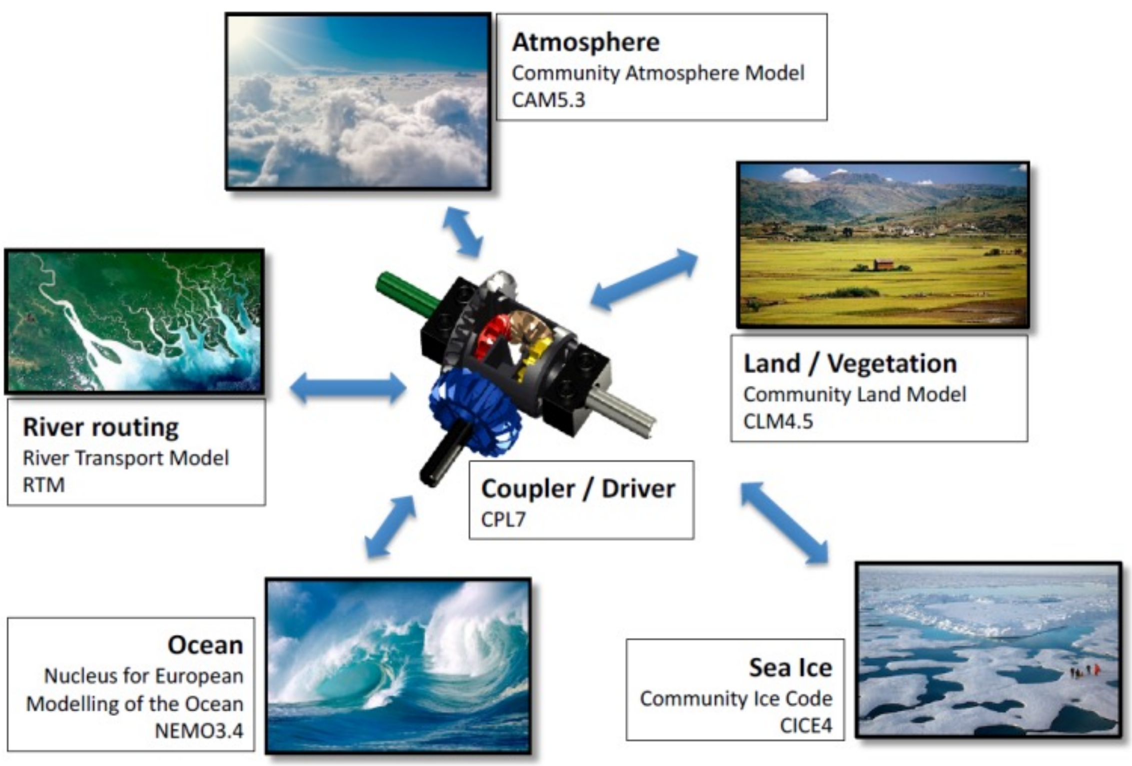

2.2 CONFIGURATION OF THE OPERATIONAL PREDICTION SYSTEM

The CMCC-SPS3.5 model consists of several independent but fully coupled model components simultaneously simulating the Earth's atmosphere, ocean, land, sea ice and river routing, together with a central coupler/driver component that controls data synchronization and exchange (see the sketch of Figure 1).

The CMCC-SPS3.5 atmospheric, land surface, sea ice and river routing model components are based on CESM, the NCAR Community Earth System Model version 1.2.2 (in their CAM5.3, CLM4.5, CICE4 and RTM versions, respectively). A detailed description of such models is given in Hurrell et al. (2013) and references therein. The ocean component is based on NEMO, the European Nucleus for European Modelling of the Ocean model, in its 3.4 version; for a detailed description, see Madec et al. (2008). For an evaluation of CMCC-SPS3 performance (bias and skill), see Sanna et al. (2017).

2.2.1 ATMOSPHERE

The atmospheric component of CMCC-SPS3.5 is the Community Atmosphere Model version 5 (CAM5.3, see Neale et al., 2010 for a description of the model macrophysics) which can be configured to use a spectral element, a finite volume, a spectral Eulerian or a spectral Semi-Lagrangian dynamical core, see Dennis et al. (2012) and Neale et al. (2010). The atmosphere implemented in CMCC-SPS3.5 is hydrostatic and uses the Spectral Element dynamical core (a formulation of the spectral element method using high-degree hybrid polynomials as base functions can be found in Patera, 1984), with a horizontal resolution of ½° (about 55 km), 46 vertical levels up to about 0.3 hPa. A Hyperviscosity term is included in order to damp the propagation of spurious grid-scale modes (Ainsworth & Wajid, 2009).

The integration time-step of the full physics is 30 minutes while, as far as the dynamical core is concerned, the time-step of the "tracer" advection is 225 seconds (1/8 of the physics time-step) and the time-step of the fluid-dynamics is 56.25 seconds (1/32 of the physics time-step).

A description of the treatment for stratiform cloud formation, condensation, and evaporation macrophysics is given in Neale et al. (2010). A two-moment microphysical parameterization (Morrison and Gettelman, 2008; Gettelman et al. 2008) is used to predict the mass and number of smaller cloud particles (liquid and ice), while the mass and number of larger-precipitating particles (rain and snow) are diagnosed. Cloud microphysics interacts with the model's greenhouse gas concentration, where observed yearly values are specified before 2005 and CMIP5 protocol concentrations (scenario RCP8.5) are used after 2005, see IPCC (2013). Differently from the standard version of CAM5.3, in CMCC-SPS3.5 (as it was also in CMCC-SPS3) the aerosol distribution does not evolve in time through the CAM modal aerosol model (MAM) but is taken from a fixed climatology (referring to year 2000). A Rapid Radiative Transfer Model for GCMs (RRTMG; Iacono et al., 2008, Bretherton et al., 2012, Liu et al., 2012) is used to calculate the radiative fluxes and heating rates for gaseous and condensed atmospheric species. A statistical technique is used to represent sub-grid-scale cloud overlap (Pincus et al., 2003). Moist turbulence (Bretherton and Park, 2009) and shallow convection parameterization schemes (Park and Bretherton, 2009) are used to simulate shallow clouds in the planetary boundary layer.

The process of deep convection is treated with a parameterization scheme developed by Zhang and McFarlane (1995) and modified with the addition of convective momentum transports by Richter and Rasch (2008) and a modified dilute plume calculation following Raymond and Blyth (1986, 1992). Moist convection occurs only when there is convective available potential energy (CAPE) for which parcel ascent from the sub-cloud layer acts to destroy the CAPE at an exponential rate using a specified adjustment time scale.

The physics package includes a parameterization of convective, frontal and orographic gravity wave drag (GWD) following McFarlane (1987), Richter et al (2010) and Richter et al. (2014). The convective GWD efficiency is adjusted to produce a QBO period in the lower stratosphere closer to observations.

The turbulent surface drag due to unresolved orography is taken into account by the Turbulent Mountain Stress (TMS) scheme. Details on this parameterization can be found in Neale et al. (2012), Richter et al. (2010) and Lindvall et al. (2016). Vertical diffusion of heat and momentum is parameterized following Bretherton and Park (2008), with the so-called “University of Washington Moist Turbulence scheme” (UWMT). Inside UWMT the effect of turbulence is represented by a down-gradient diffusion term.

This version of CAM5 uses a modified vertical grid that with 46 vertical levels and a model top at 0.3 hPa.

The increase of atmospheric model resolution from 1° (SPS3) to ½° (SPS3.5) required not only a change of the dynamical core time-step, but also a readjustment (retuning) of surface friction, vertical diffusion and GWD control parameters as outlined below in Sect. 2.5.2.

Atmospheric Model:	CAM5.3
Dynamics:	Hydrostatic, based on a continuous Galerkin spectral finite-element method (basis functions: high degree hybrid polynomials).
Physics:	Deep moist convection, stratiform clouds, condensation and evaporation macrophysics, two-moment microphysical parameterization (liquid and ice), orographic, frontal and convective GWD, surface friction and free-atmosphere vertical diffusion. Rain and snow diagnosed, cloud

	microphysics-GH gases interaction (GH gases concentration prescribed),
	RRTMG Rapid Radiative Transfer Model, sub-grid-scale cloud overlap, moist turbulence and shallow convection in PBL.
Horizontal resolution and grid:	1/2° approx., cube-sphere quasi-regular grid.
Vertical resolution:	46 vertical levels.
Top-of-the-atmosphere:	0.3 hPa (60 km approx.).
Main Physics Time-step:	30 minutes.
“Tracer” Advection Time-step:	225 seconds (1/8 of the Physics time-step)
Fluid-Dynamics Time-step:	56.25 seconds (1/32 of the Physics time-step).

2.2.2 THE RETUNING OF OROGRAPHIC GWD, SURFACE FRICTION AND VERTICAL DIFFUSION FOLLOWING THE DOUBLING OF THE ATMOSPHERIC MODEL HORIZONTAL RESOLUTION

Due to the doubling of the atmospheric model horizontal resolution, some minor re-tuning of some physical parametrizations of the atmospheric model was considered useful in order to reduce the model bias, mostly on lower and mid-tropospheric dynamical fields. The re-tuning was performed based on the results of a number of 5-year AMIP-like simulations (1981-1985), where the atmospheric model was forced by observed SST and sea-ice conditions. It was decided to focus this re-tuning effort on three parameterizations of orographic GWD, surface friction (over land) and vertical diffusion. The main outcomes of this effort are reported in the following sub-sections.

2.2.2.1 OROGRAPHIC GRAVITY-WAVE DRAG (OGWD)

CAM5 OGWD is parameterized following McFarlane (1987) and Neale et al. (2012). First of all, the magnitude of the vertical flux of horizontal momentum at the source level is diagnosed; then, the vertical profile of momentum flux is calculated. At those levels where the saturation of the wave occurs, the drag effect on the atmosphere is realized by calculating and adding to the flow the OGWD horizontal wind tendency. The value of this tendency is modulated by the efficiency parameter effgw_oro; its standard value is 0.0625. After the tuning experiments, it was decided to increase effgw_oro by a factor 2.5: in SPS3.5, effgw_oro = 0.15625.

2.2.2.2 SURFACE FRICTION

In CAM5, the turbulent surface drag due to unresolved orography is taken into account by the Turbulent Mountain Stress (TMS) scheme. Details on this parameterization can be found in Neale et al. (2012), Richter et al. (2010) and Lindvall et al. (2016). The surface stress is is calculated from the wind vector, air density and a drag coefficient, which depends on an effective roughness length factor z0, representing the unresolved orography. In particular, it establishes the minimum roughness length seen by the model. Its maximum value is fixed to 100 m, while its minimum value is the standard deviation of the subgrid orography multiplied by the tms_z0fac parameter. The standard value of tms_z0fac is 0.075. After the tuning experiments, it was decided to set tms_z0fac = 0.1875, therefore increasing it by a factor of 2.5.

2.2.2.3 VERTICAL DIFFUSION

In CAM5, vertical diffusion of heat and momentum is controlled by the Bretherton and Park (2008) parameterization scheme, the so-called “University of Washington Moist Turbulence” scheme (UWMT). Inside UWMT, the effect of turbulence is represented by down-gradient diffusion. Diffusion between two adjacent model levels is activated only if the interface between them is classified as turbulent on the basis of the Richardson Number. Turbulent interfaces are diagnosed using the local Richardson number Ri : in the standard (SPS3.5) configuration, if Ri<Ri_crit=0.19, the interface is assumed to be turbulent and vertical diffusion happens. After the tuning experiments, it

was decided to double Ri_crit, setting Ri_crit = 0.4, allowing therefore for more vertical diffusion.

2.2.2.4 MEAN MAPS AND BIASES OF MSLP AND 500 HPA FOR WINTER AND SUMMER

OGWD, surface friction and vertical diffusion all have influence on vertical momentum (and energy) transport, which means that they strongly interact non linearly with each other via changing the mean flow. They could not, therefore, be re-tuned singularly. Several combinations of the three parametrization settings were tried until a satisfactory set of new parameters was achieved, showing noticeable overall improvements in comparison with both the old SPS3 maps and the un-tuned SPS3.5 maps (see the following Figures 2 to 9).

Only the maps referring to the final re-tuned combination are shown here, i.e. the maps comparing results obtained with SPS3, SPS3.5 before and after the tuning, and data from ERA5 reanalysis for the same period, for both Winter (DJF) and Summer (JJA).

Figure 2: Winter (DJF) Mean Sea Level Pressure for SPS3, SPS3.5 before the tuning (SPS3.5 - BT), SPS3.5 in its final configuration and ERA5.

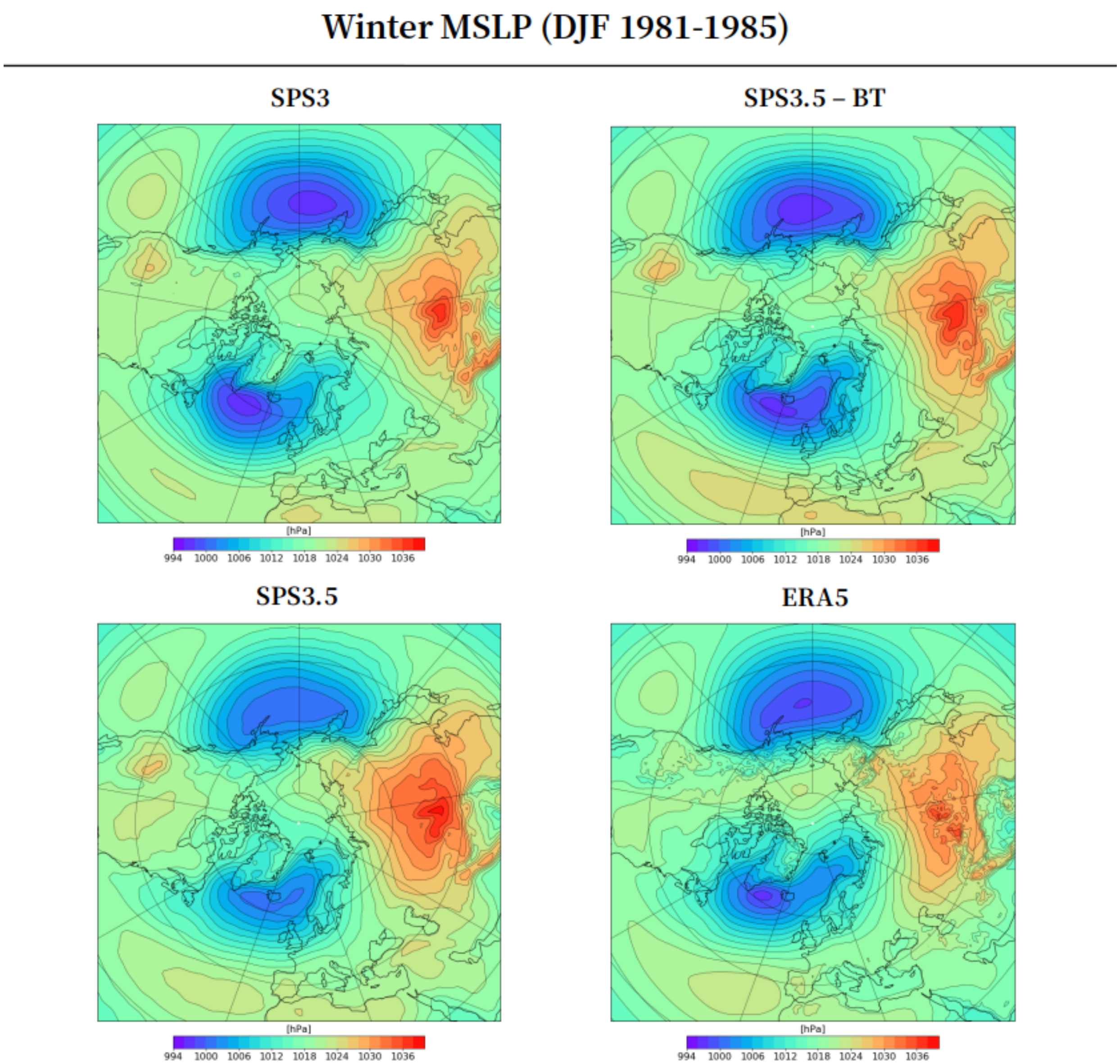

Figure 3: Winter (DJF) Mean Sea Level Pressure bias for SPS3, SPS3.5 before the tuning (SPS3.5 - BT), SPS3.5 in its final configuration and ERA5.

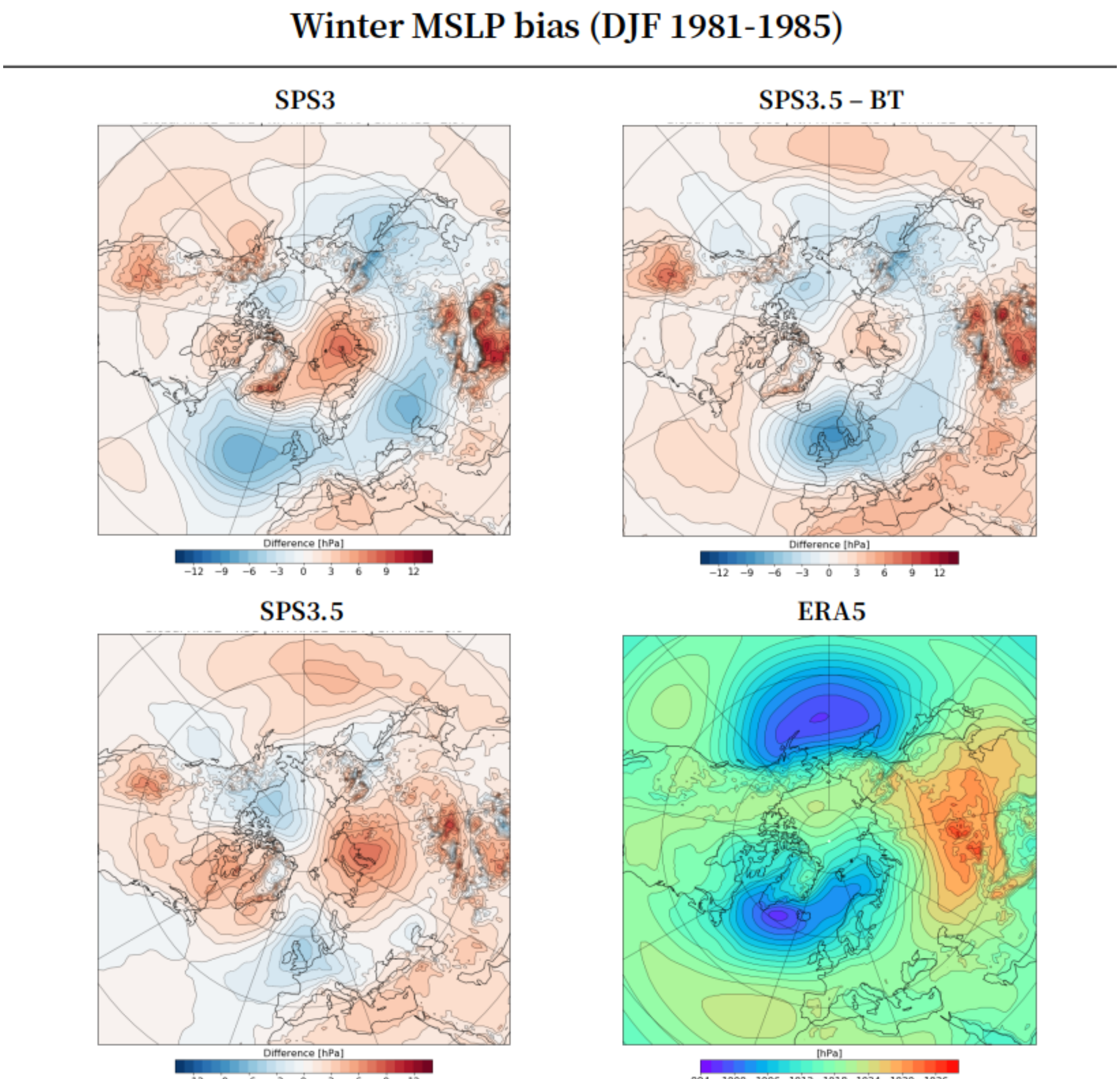

Figure 4: Winter (DJF) 500 hPa geopotential height for SPS3, SPS3.5 before the tuning (SPS3.5 - BT), SPS3.5 in its final configuration and ERA5.

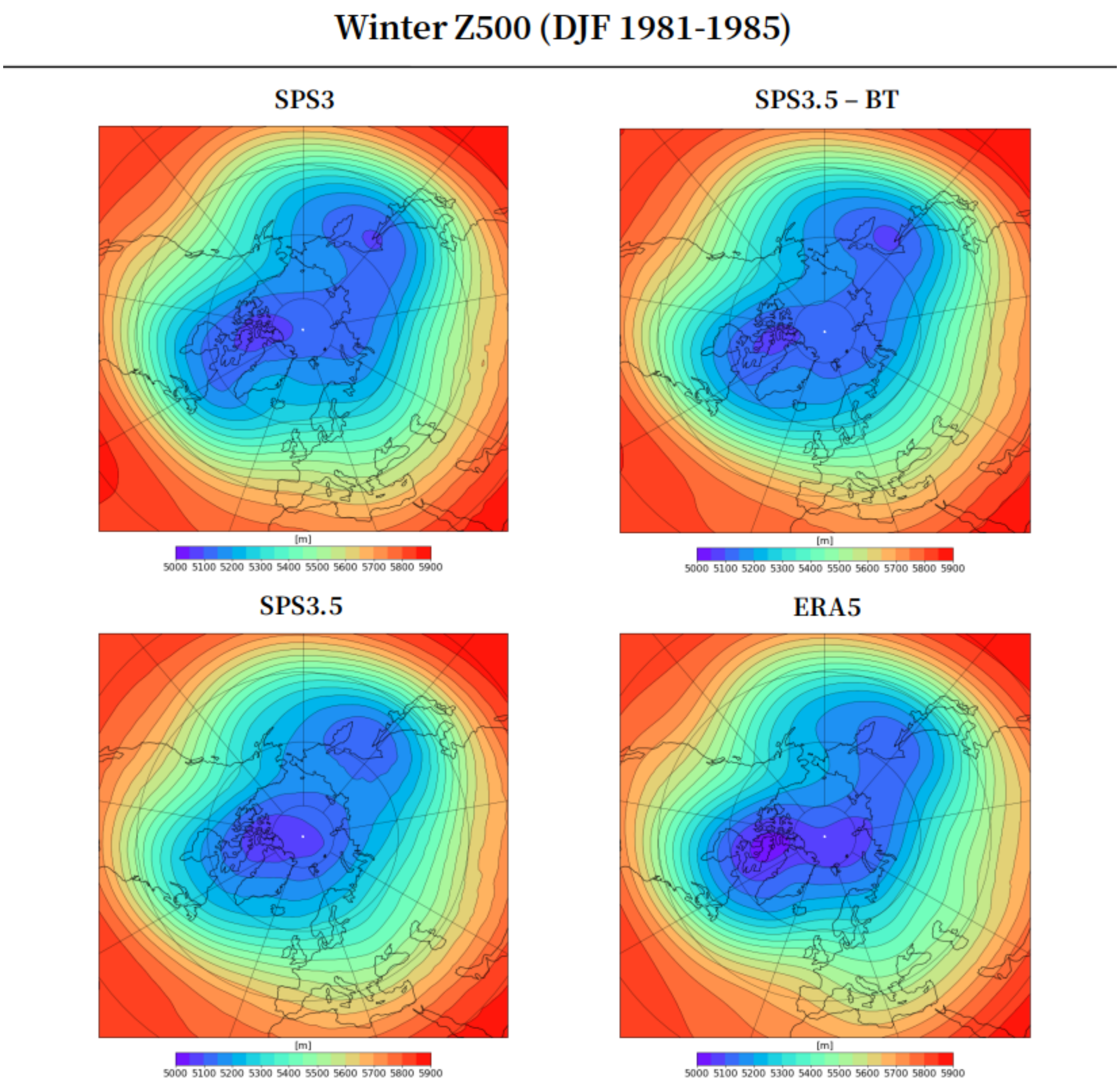

Figure 5: Winter (DJF) 500 hPa geopotential height bias for SPS3, SPS3.5 before the tuning (SPS3.5 - BT), SPS3.5 in its final configuration and ERA5.

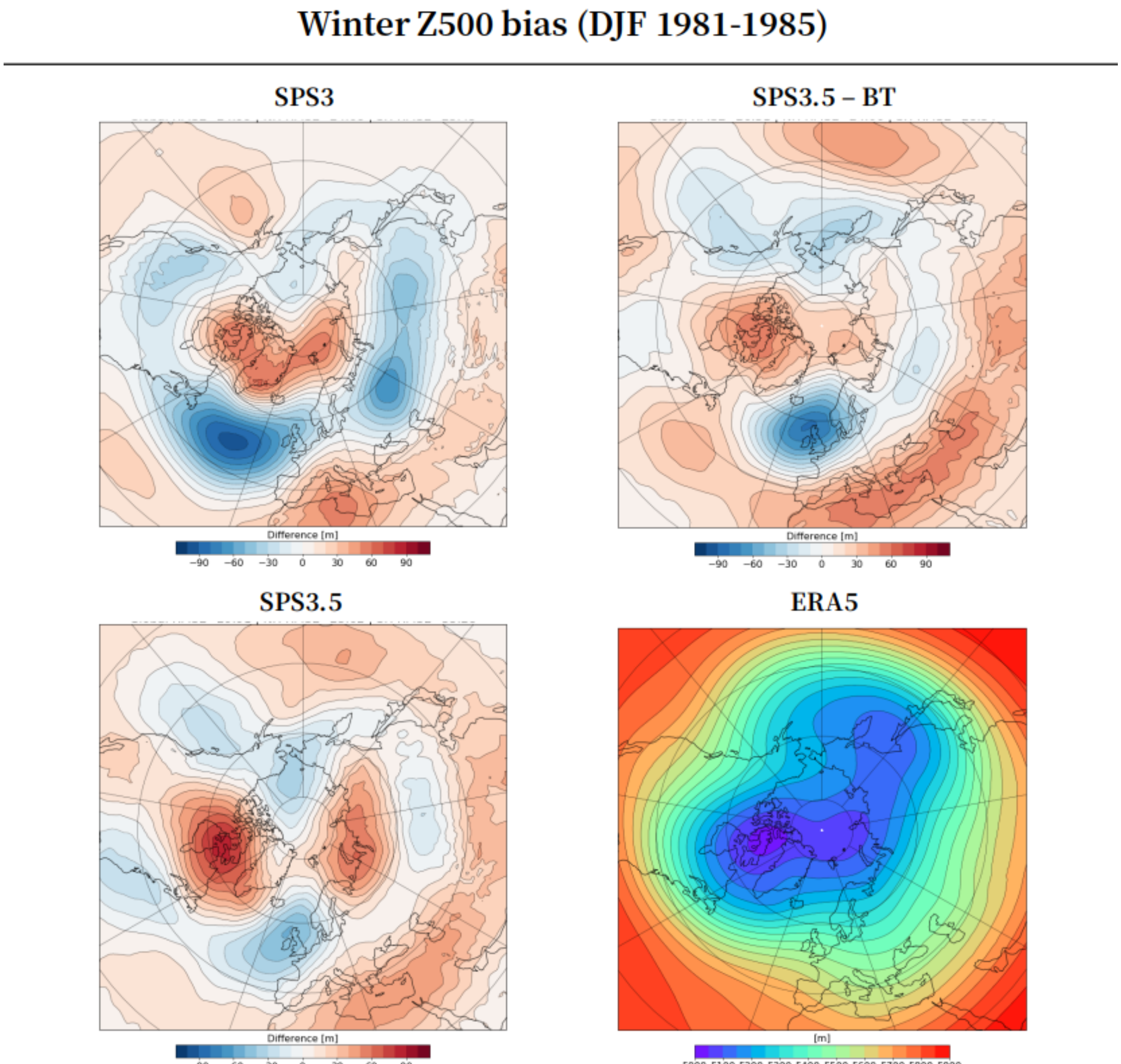

Figure 6: Summer (JJA) Mean Sea Level Pressure for SPS3, SPS3.5 before the tuning (SPS3.5 - BT), SPS3.5 in its final configuration and ERA5.

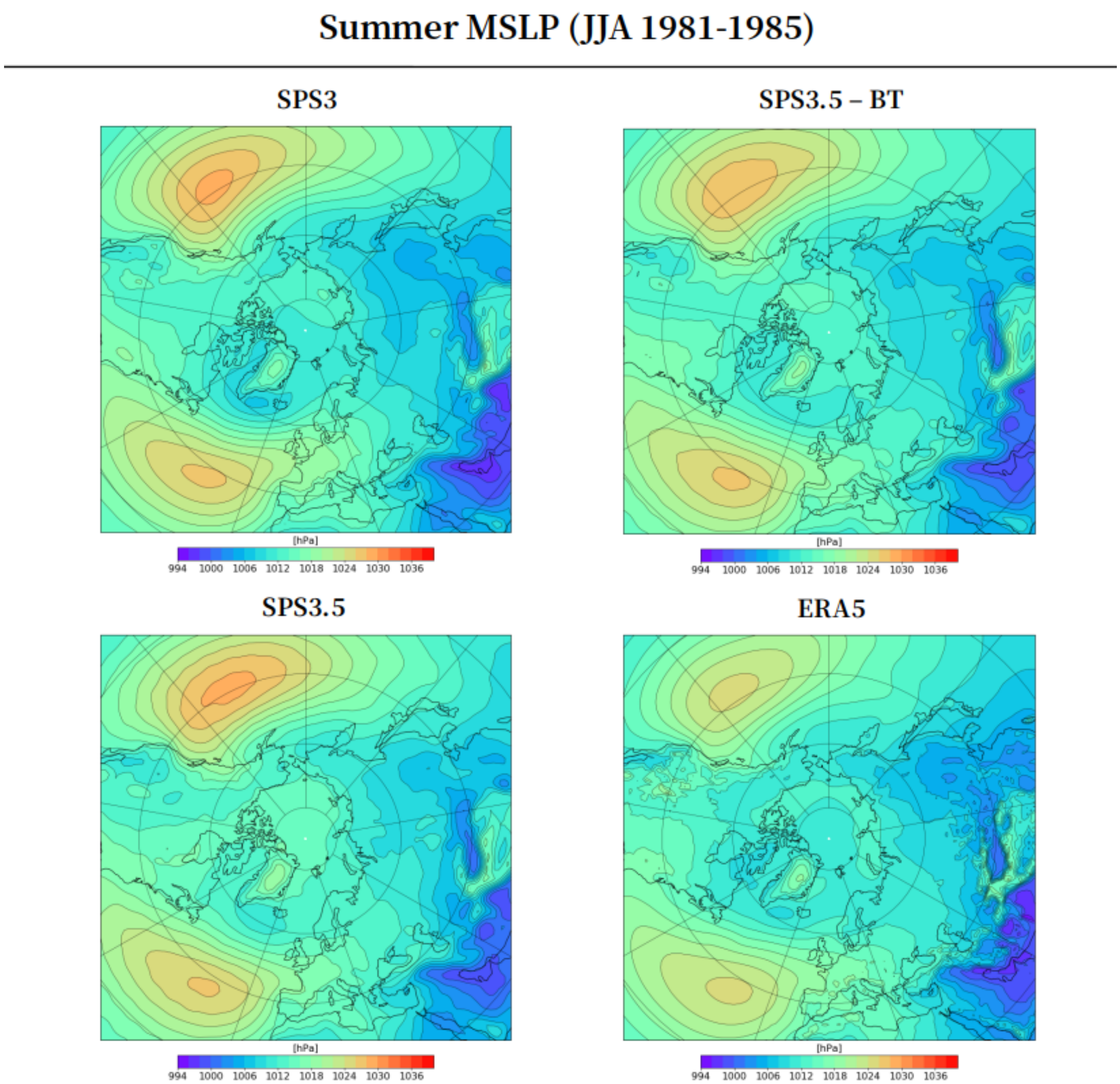

Figure 7: Summer (JJA) Mean Sea Level Pressure bias for SPS3, SPS3.5 before the tuning (SPS3.5 - BT), SPS3.5 in its final configuration and ERA5.

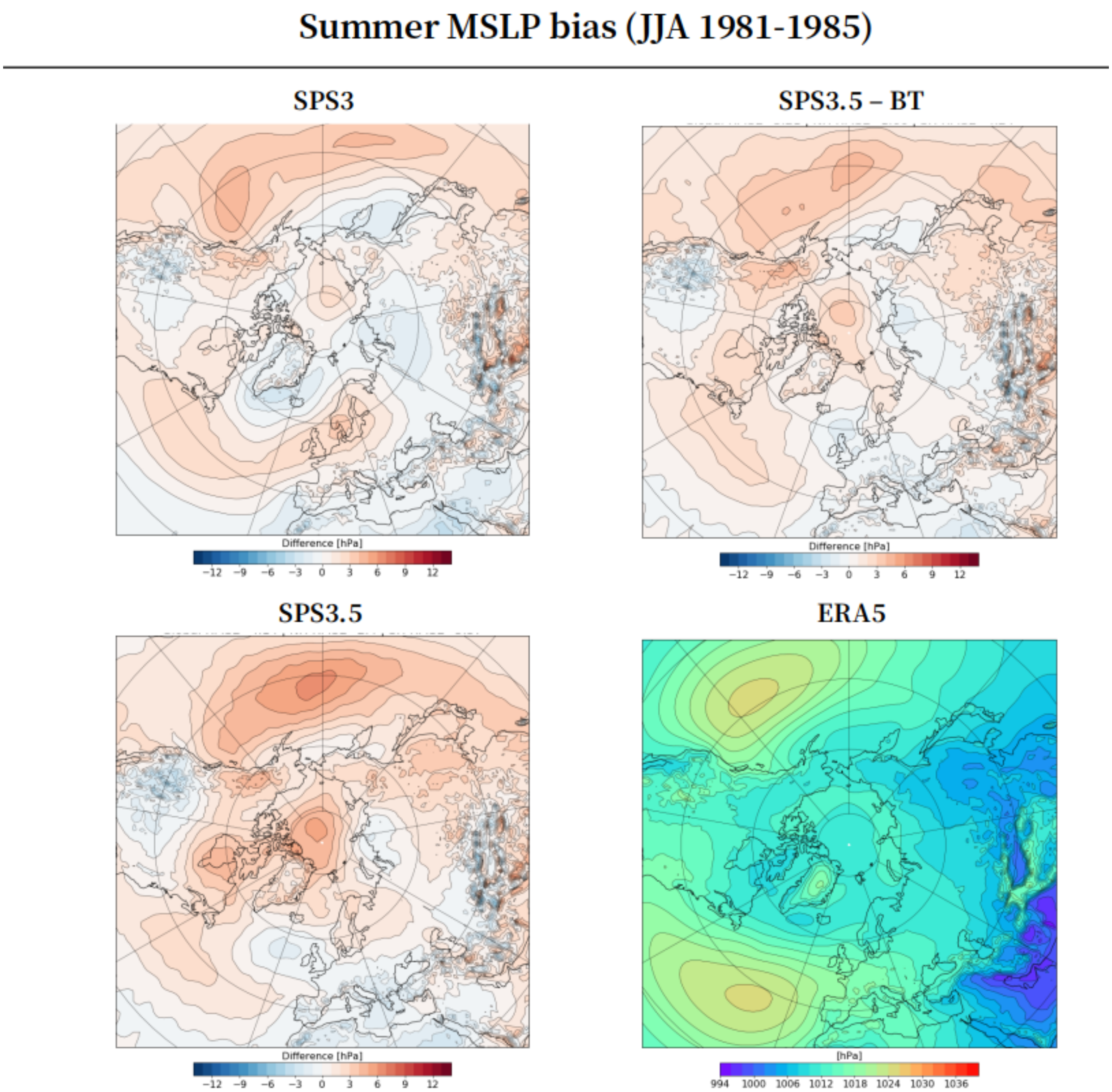

Figure 8: Summer (JJA) 500 hPa geopotential height for SPS3, SPS3.5 before the tuning (SPS3.5 - BT), SPS3.5 in its final configuration and ERA5.

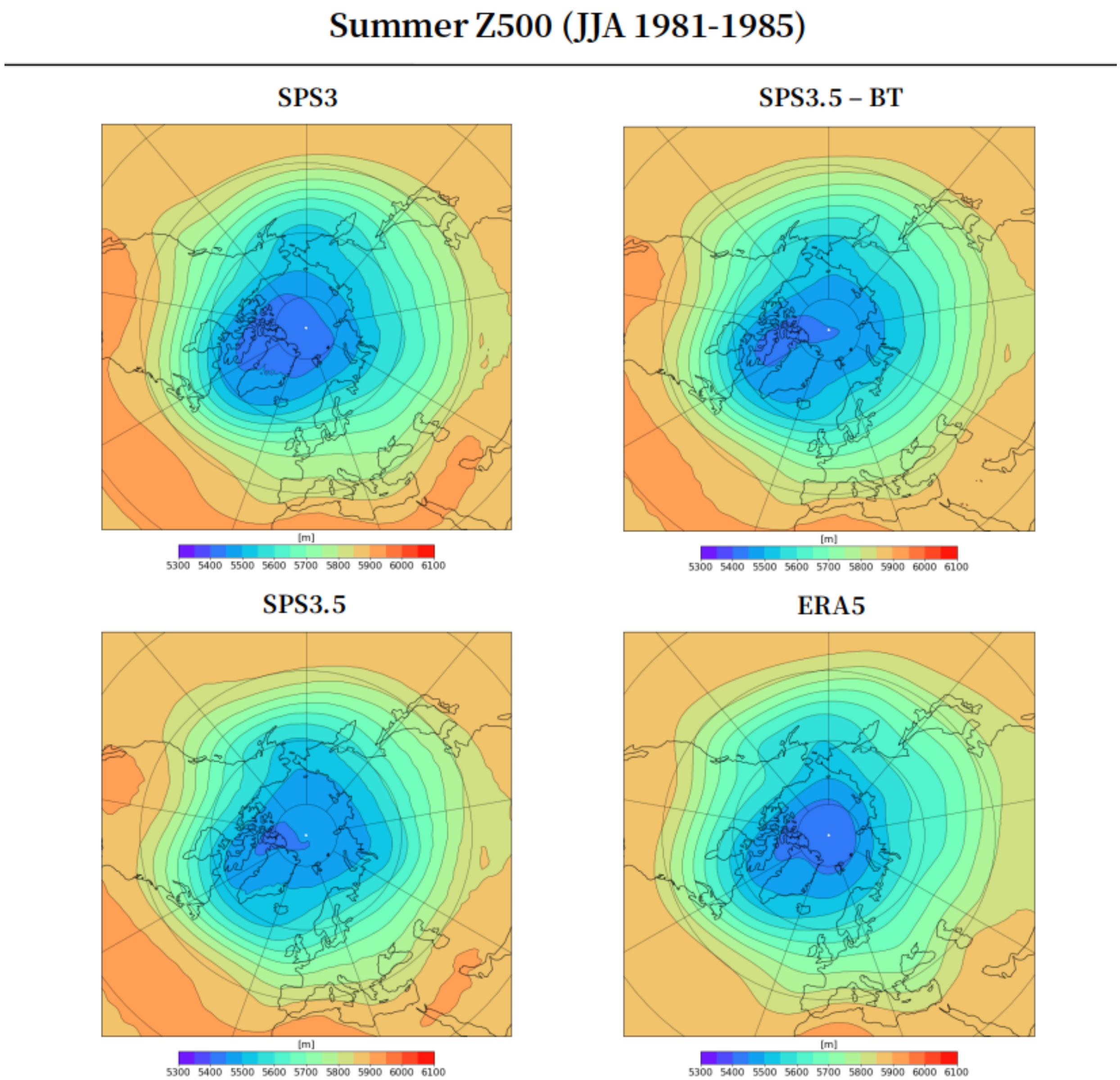

Figure 9: Summer (JJA) 500 hPa geopotential height bias for SPS3, SPS3.5 before the tuning (SPS3.5 - BT), SPS3.5 in its final configuration and ERA5.

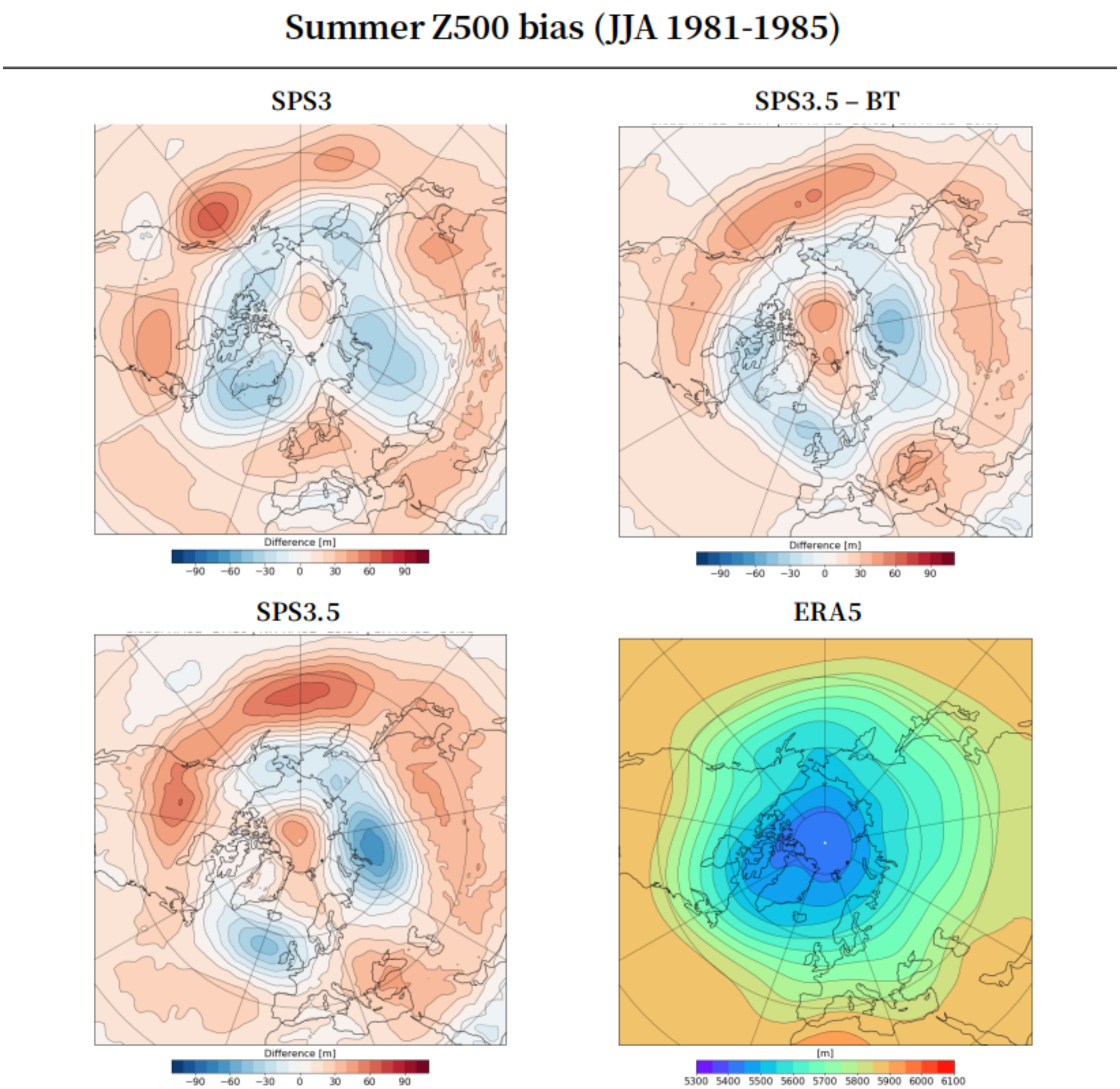

2.2.3 OCEAN

The Nucleus for European Modelling of the Ocean (NEMO) is the ocean model of CMCC-SPS3.5. The NEMO model solves the primitive equations subject to the Boussinesq, hydrostatic and incompressibility approximations. The prognostic variables are the three velocity components, the sea surface height, the potential temperature and the practical salinity.

The ocean component used in CMCC-SPS3.5 is based on the eddy-permitting Version 3.4 of NEMO, with a horizontal resolution of about 25 km, 50 vertical levels (31 in the first 500 m) and an integration time-step of 18 minutes.

In the horizontal, the model uses a nearly isotropic, curvilinear, tri-polar, orthogonal grid with an Arakawa C–type three-dimensional arrangement of variables. The model is integrated in its eddy-permitting, 1/4° resolution configuration. In the vertical, a partial step z-coordinate is used.

The model uses a filtered, linear, free-surface formulation, where lateral water, tracers and momentum fluxes are calculated using fixed-reference ocean surface height. The time integration scheme used is a Robert–Asselin filtered leapfrog for non-diffusive processes and a forward (backward) scheme for horizontal (vertical) diffusive processes (Griffies, 2004). The linear free-surface is integrated in time implicitly using the same time step.

NEMO uses a non-linear equation of state. Tracers advection uses a Total Variance Dissipation (TVD) scheme while momentum advection is formulated in vector invariant form, using an energy and enstrophy conserving scheme (Zalesak, 1979). The vertical turbulent transport is parameterized using a Turbulent Kinetic Energy (TKE) closure scheme (Gaspar et al., 1990) plus parameterizations of double diffusion, Langmuir cell and surface wave breaking. An enhanced vertical diffusion parameterization is used in regions where the stratification becomes unstable. Tracers' lateral diffusion uses a diffusivity coefficient scaled according to the grid spacing, while lateral viscosity makes use of a space-varying coefficient. Both are parameterized by a horizontal bi-Laplacian operator. Free-slip boundary conditions are applied at the ocean lateral boundaries. At the ocean floor, a bottom intensified tidally-driven mixing (Simmons et al., 2004), a diffusive bottom boundary layer scheme and a nonlinear bottom friction are applied. No geothermal heat flux is applied through the ocean floor. The shortwave radiation from the atmosphere is absorbed in the surface layers using RGB chlorophyll-dependent attenuation coefficients. No wave model is included.

Ocean model:	NEMO v3.4.
Dynamics:	Hydrostatic. Filtered, linear, free-surface formulation; lateral water, tracers and momentum fluxes calculated using fixed-reference ocean surface height. Non-linear equation of state. Total Variance Dissipation (TVD) scheme for Tracers advection. Momentum advection formulated in vector invariant form with energy and enstrophy conserving scheme.
Physics	Enhanced vertical diffusion parameterization in regions where stratification becomes unstable Tracers' lateral diffusion with diffusivity coefficient scaled according to grid spacing. Diffusive bottom boundary layer scheme and nonlinear bottom friction.
Horizontal resolution and grid:	1/4° approx., nearly isotropic, curvilinear, tri-polar, orthogonal grid.
Vertical resolution:	50 vertical levels.
Time step:	18 minutes.

2.2.4 SEA ICE

The sea ice component is version 4 of the Community Ice CodE (CICE4, Hunke et al., 2010) which uses the same horizontal grid of the ocean model, but an integration timestep of 30 minutes. It includes the thermodynamics of Bitz and Lipscomb (1999), the elastic–viscous–plastic dynamics of Hunke and Dukowicz (1997). The sea ice model also contains a multiple scattering shortwave radiation treatment (Briegleb and Light, 2007, Holland et al., 2012) and associated capabilities to simulate explicitly melt-pond evolution and the deposition and cycling of aerosols (dust and black carbon) within the ice pack. In the CMCC-SPS3.5 configuration, however, only one sea ice vertical layer (ice thickness) is used.

Sea ice model:	CICE4.
Horizontal resolution and grid:	1/4°, grid same as ocean model.
Sea ice model layers:	1 (thickness only).
Timestep:	30 min.

2.2.5 LAND SURFACE

The land component of the CMCC-SPS3.5 forecast system is the Community Land Model (CLM4.5, Oleson et al., 2013). CLM4.5 runs at the same resolution as the atmospheric model (about 1/2°), with a 30-minute time-step. The configuration incorporated in CMCC-SPS3.5 (the so-called Satellite Phenology version of CLM4.5) allows only a simplified vegetation dynamics, which includes a treatment of mass and energy fluxes associated with prescribed temporal (seasonal) change in land cover due to LAI (Leaf Area Index) but not to Plant Functional Types (PFTs), which are kept constant in time during the six-month integration. No evolving biosphere or crop model are therefore present and plant phenology (LAI) is determined through a prescribed seasonally-dependent satellite climatology.

The snow model incorporates the Snow, land-Ice and Aerosol Radiation (SNICAR) model (Flanner et al. 2007). SNICAR includes aerosol deposition of black carbon and dust, grain-size dependent snow aging, and vertically resolved snowpack heating. A perched water table above icy permafrost ground is also present (Swenson et al., 2012).

The lake model has a representation of surface water (Subin et al., 2012), permitting prognostic wetland distribution. The energy fluxes are calculated separately for snow/water-covered and snow/water-free land and glacier units.

Soil levels: 10.

Horizontal resolution: same as atmospheric model, i.e. 1/2x1/2° approximately.

Timestep: 30-minute.

2.2.6 RIVER ROUTING

The RTM (River Transport Model) routes total runoff from the land surface model to either the active ocean, or to marginal seas with a design that enables the hydrologic cycle to be closed (Branstetter, 2001; Branstetter and Famiglietti, 1999). The horizontal resolution is half-degree (about 50km) and the integration time-step is three-hourly.

2.2.7 THE COUPLER

All system components are synchronized by the CESM coupler/driver (CPL7, Craig et al., 2011). The coupling architecture provides plug-and-play capability of data and active components.

Coupling frequencies:

Atmosphere-Ocean: 90 minutes (every third time-step of the atmospheric model).

Atmosphere-Land: 30 minutes (every time-step of the atmospheric model).

Atmosphere-Sea Ice: 30 minutes (which is the same time-step of the atmospheric model).

2.3 ATMOSPHERIC MODEL GRIDS, OCEAN MODEL GRIDS AND POST-PROCESSING GRIDS

2.3.1 THE HORIZONTAL AND VERTICAL GRIDS OF CAM5.3

The atmospheric model's horizontal grid is the so-called Cubed-Sphere grid (see Figure 10) first used

in Sadourny (1972). Each cube face is mapped to the surface of the sphere with the equal-angle gnomonic projection (Rancic et al., 1996). The vertical grid/coordinate is an eta-type coordinate, following Simmons and Burridge (1981). The horizontal resolution is about 55 km and the model has 46 vertical levels, up to about 0.3 hPa.

Figure 10: Tiling the surface of the sphere with quadrilaterals. An inscribed cube is projected to the surface of the sphere. The faces of the cubed sphere are further subdivided to form a quadrilateral grid of the desired resolution. Coordinate lines from the gnomonic equal-angle projection are shown, see e.g. Sadourny (1972).

2.3.2 THE HORIZONTAL AND VERTICAL GRIDS OF NEMO

In this operational, global configuration, NEMO uses, in the horizontal, an ORCA-family, curvilinear, tripolar, orthogonal grid (based on Mercator projection), which has a pole in the Southern Hemisphere, collocated with the geographic South Pole, and two poles placed on land in the Northern Hemisphere (in Siberia and Canada), in order to overcome the Pole singularities.

Figure 11: ORCA mesh conception. The departure from an isotropic Mercator grid start poleward of 20. The two "north pole" are the foci of a series of embedded ellipses (blue curves) which are determined analytically and form the i-lines of the ORCA mesh (pseudo latitudes). Then, following Madec and Imbard (1996), the normal to the series of ellipses (red curves) is computed which provide the j-lines of the mesh (pseudo longitudes).

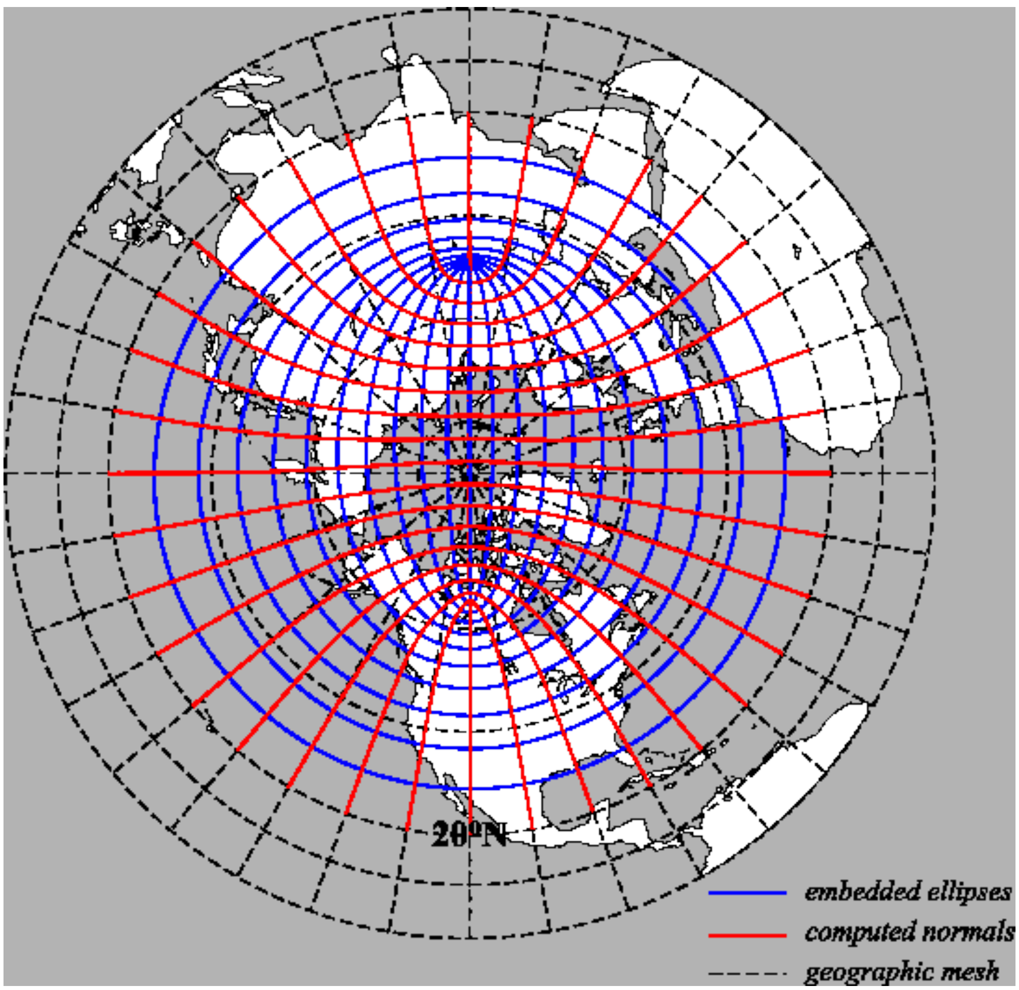

The ORCA grid is based on the semi-analytical method of Madec and Imbard (1996). It allows to construct a global orthogonal curvilinear ocean mesh, which has no singularity point inside the computational domain, since two north mesh poles are introduced, in addition to the South Pole, and placed on land. The method involves defining an analytical set of mesh parallels in the stereographic polar plan, computing the associated set of mesh meridians and projecting the resulting mesh onto the sphere. The set of mesh parallels used is a series of embedded ellipses which foci are the two mesh north poles (see Figure 11). The resulting mesh presents no loss of continuity in either the mesh lines or the scale factors, or even the scale factor derivatives over the whole ocean domain, as the mesh is not a composite mesh. Poleward of 20°N, the two NH poles introduce a weak anisotropy over the ocean areas.

In the vertical, a partial step z-coordinate is used.

The horizontal resolution of the tri-polar grid is approximately 25 km and the ocean model has 50 vertical levels (31 in the first 500 m).

2.3.3 POST-PROCESSING OUTPUT GRID AND RE-GRIDDING METHODS

The final output data are gridded on a regular lat-lon grid of 1x1°. Three-dimensional variables are provided on Standard Pressure Levels in the vertical. Surface fields are provided on the model's orography, which is also an output field.

Re-gridding is performed through the ESMF package of NCL for CAM, CICE and NEMO. For CLM a re-gridding package included in CESM is used (for more information, see Sect. 2.6).

2.4 INITIAL CONDITIONS, INITIAL CONDITION PERTURBATIONS AND MODEL UNCERTAINTY PERTURBATIONS

2.4.1 ATMOSPHERIC INITIAL CONDITIONS AND PERTURBATIONS

Atmospheric Initial Conditions (ICs) for operational forecasts are provided by ECMWF operational IFS 00UTC analyses for the first of the month as extracted from the MARS database on a regular lat-lon grid at ½° resolution. They are then interpolated onto the model quasi-regular cubed-sphere grid.

Nine further perturbed atmospheric initial conditions are obtained by applying a time-lagging technique, that is using previous ECMWF analyses at 12 hour intervals up to 5 days before. Before forecast integration, all time-lagged initial conditions are integrated for 12, 24, 36…hours, and so on up to 00UTC of the first of the month. This procedure finally provides 10 alternative atmospheric initial conditions from 00UTC of the first day of the month, all of them with superimposed perturbations of all model prognostic field variables provided by short-to-medium-range (12h up to 5 days) forecast errors.

In the case of hindcasts, ECMWF operational analyses are substituted by ERA5 analyses (Hersbach et al., 2020).

	Hindcasts	Forecasts
Atmosphere initialization	ERA5	ECMWF IFS operational
Atmosphere IC perturbations	10	10

2.4.2 LAND INITIAL CONDITION AND PERTURBATIONS

Land initial conditions are obtained from a one-month run ending on forecast initial date, forced by an observed atmosphere. This forced run is, in turn, initialized from a fixed 20-year spin-up run. Soil moisture and snow fields are also initialized from the same one-month forced run.

In order to generate three alternative land initial conditions, perturbations are obtained by using in turn analyses from ECMWF, NCEP and the mean of the two as forcing observed atmosphere. This provides three land initial conditions. In the case of operational forecasts, the observed atmosphere is provided by ECMWF operational analyses or by NCEP re-analyses or by a mean of both. In the case of hindcasts, the observed atmosphere is provided by ECMWF ERA5 (Hersbach et al., 2020) or by

NCEP re-analyses (Kalnay et al., 1996), or by a mean of both. This yields three possible initial conditions for the land surface.

For more ECMWF or NCEP Data Assimilation method details, see Sect. 2.6.

	Hindcasts	Forecasts
Land Initialization	Forced (obs. atmosphere) monthly run initialized from 10-year spin-up	Forced (obs. atmosphere) monthly run initialized from 10-year spin-up
Land IC perturbations	3	3
Soil moisture initialization	From land initialization	From land initialization
Snow initialization	From land initialization	From land initialization

2.4.3 OCEAN INITIAL CONDITION AND PERTURBATIONS

Ocean Initial Conditions are obtained by a 3D-VAR intermittent ocean data assimilation cycle performed with C-GLORS. Perturbations of initial conditions are obtained by re-assimilating observed data after insertion of added random perturbations on Sea-Level Anomalies (SLA) and on In-Situ profile observations of temperature and salinity (Burgers et al., 1998) and by perturbing the atmospheric fluxes and the ocean model equation of state (EOS) for seawater, during the integration of the assimilating model (Brankart, 2013). No unperturbed control forecast is used for the ocean model.

	Hindcasts	Forecasts
Ocean initialization	C-GLORS Global Ocean 3D-VAR	C-GLORS Global Ocean 3D-VAR
Ocean IC perturbations	4	8

2.4.4 SEA-ICE INITIAL CONDITION AND PERTURBATIONS

In order to produce Sea-Ice Initial Conditions, observed data of sea-ice concentration (SIC) and sea-ice-thickness (SIT) are assimilated, using on-line nudging schemes with a relaxation time scale of 8 hours and 5 days respectively. The observed SIC field is downloaded from the National Snow and Ice Data Center (NSIDC) (Cavalieri et al., 1999), while the SIT is constrained towards PIOMAS data (Pan-Arctic Ice Ocean Modeling and Assimilation System, Zhang and Rothrock, 2003) available for the Arctic area.

The assimilation of SIC and SIT data is performed during the C-GLORS ocean data-assimilation system, where, however, the LIM2 ice model within the NEMO ocean model substitutes the CICE4 used during coupled forecast integration. The LIM2 sea ice is the Louvain-la-Neuve Sea Ice Model (Fichefet and Morales Maqueda, 1997) which includes the representation of both thermodynamic and dynamic processes. The ice dynamics are calculated according to external forcing generated from wind stress, ocean stress and sea-surface tilt and to internal ice stresses. Internal ice stresses are computed using the elastic viscous-plastic (EVP) formulation of ice dynamics by Hunke and Dukowicz (1997) on a C-grid (Bouillon, Maqueda, Legat, and Fichefet, 2009).

No ice data are perturbed during data assimilation, however slightly different sea-ice data can be produced by the ocean data multiple perturbation procedure which generates the 8 alternative ocean initial conditions (4 for hindcasts). No Model dynamics or physics perturbations are applied to the sea-ice model and there is no special control forecast.

2.4.5 COMBINATION AND CHOICE OF PERTURBED INITIAL CONDITIONS TO GENERATE THE ENSEMBLE

The 10 atmospheric perturbed ICs, the 3 land perturbed ICs and the 8 (4 in hindcast mode) ocean perturbed ICs are combined to yield 240 (120 in hindcast mode) possible perturbed ICs among which the 50 ICs (40 ICs in hindcast mode) to produce the forecast ensemble are chosen at random.

2.5 FORECAST AND HINDCAST ENSEMBLE SIZE AND AVAILABLE INITIAL DATES

Forecast ensemble size	50 members
Hindcast ensemble size	40 members
Hindcast time coverage	1/1993-12/2016 with both SPS3 and SPS3.5
Pre-Operational Forecast time coverage	1/2017-3/2018 with SPS3
Operational Forecasts time coverage	4/2018-9/2020 with SPS3, 10/2020-present with SPS3.5

2.6 WHERE TO FIND MORE INFORMATION

More detailed documentation on CAM Model at:
http://www.cesm.ucar.edu/models/cesm1.2/cam/

More detailed documentation on CLM Model at:
http://www.cesm.ucar.edu/models/cesm1.2/clm/

More detailed documentation on NEMO Model at:
https://www.nemo-ocean.eu/doc/

More ocean data assimilation details available at:
http://c-glors.cmcc.it/index/index.html

More DA details in ECMWF operational analysis documentation at:
https://www.ecmwf.int/en/elibrary/16666-part-ii-data-assimilation

More DA details in NCEP operational analysis and reanalyses documentation at:
https://www.esrl.noaa.gov/psd/data/gridded/data.ncep.reanalysis2.html

Documentation on the system's/models' climatology and performance can be found at:
https://www.cmcc.it/it/publications/rp0285-cmcc-sps3-the-cmcc-seasonal-prediction-system-3

More detailed documentation on the ESMF package of NCL at:
https://www.ncl.ucar.edu/Applications/ESMF.shtml

More detailed documentation on the re-gridding package included in CESM at:
http://www.cesm.ucar.edu/models/cesm1.2/clm/models/lnd/clm/doc/UsersGuide/book1.html

ACKNOWLEDGEMENTS

This work has been done in the framework of the Copernicus Climate Change Service (C3S) contract number 2018/C3S_330_CMCC

BIBLIOGRAPHY

Ainsworth, M., & Wajid, H. A. (2009). Dispersive and dissipative behavior of the spectral element method. *SIAM Journal on Numerical Analysis*, *47*(5), 3910–3937. https://doi.org/10.1137/080724976

Bitz, C. M., and Lipscomb, W. H. (1999). A new energy-conserving sea ice model for climate study. J. Geophys. Res, 104(15), 669-15.

Brankart, J.-M. (2013). Impact of uncertainties in the horizontal density gradient upon low resolution global ocean modelling. Ocean Modell. 66, 64–76. DOI: https://doi.org/10.1016/j.ocemod.2013.02.004

Branstetter, M.L., and James S. Famiglietti (1999). Testing the sensitivity of GCM-simulated runoff to climate model resolution using a parallel river transport algorithm. Proceedings of 14th Conference on Hydrology, American Meteorological Society, Dallas, Texas.

Branstetter, M.L. (2001). Development of a parallel river transport algorithm and applications to climate studies. University of Texas.

Bretherton, C. S., and S. Park (2009). A new moist turbulence parameterization in the community atmosphere model, J. Climate, *22*, 3422–3448, 2009*a*.

Bretherton, C.S., M. G. Flanner, and D. Mitchell (2012). Toward a minimal representation of aerosols in climate models: description and evaluation in the Community Atmosphere Model CAM5. Geosci. Model Dev., 5(3):709–739, 2012. doi: 10.5194/gmd-5-709-2012.

Briegleb, B. P., & Light, B. (2007). A Delta-Eddington multiple scattering parameterization for solar radiation in the sea ice component of the Community Climate System Model. NCAR Tech. Note NCAR/TN-472+ STR, 100.

Bouillon, S., M.M. Maqueda, V. Legat, and T. Fichefet. (2009) An elastic-viscousplastic sea ice model formulated on Arakawa b and c grids. Ocean Modelling, 27:174–184.

Burgers, G., van Leeuwen, P.J., Evensen, G. 1998. Analysis scheme in the ensemble Kalman filter. Mon. Weather Rev. 126, 1719–1724. http://dx.doi.org/10.1175/1520-0493(1998)126<1719:ASITEK>2.0.CO;2.

Cavalieri, D. J., Parkinson, C. L., Gloersen, P., Comiso, J. C., and Zwally, H. J. (1999). Deriving long-term time series of sea ice cover from satellite passive-microwave multisensor data sets, J. Geophys. Res., 104, 15803–15814, doi:10.1029/1999JC900081.

Craig, A. P., Vertenstein, M., & Jacob, R. (2011). A new flexible coupler for earth system modeling developed for CCSM4 and CESM1. International Journal of High Performance Computing Applications, 1094342011428141.

Dennis, J.M. et al. (2012). “CAM-SE: A scalable spectral element dynamical core for the Community Atmosphere Model”. In: The International Journal of High Performance Computing Applications 26.

Fichefet T. and M.A. Morales Maqueda (1997). Sensitivity of a global sea ice model to the treatment of ice thermodynamics and dynamics. Journal of Geophysical Research, 102:12609–12646, 1997.

Flanner, M.G., et al. (2007). Present-day climate forcing and response from black carbon snow. Journal of Geophysical Research: Atmospheres. 112, D11.

Gaspar, P., Y. Gregoris, and J.-M. Lefevre (1990). A simple eddy kinetic energy model for simulations of the oceanic vertical mixing Tests at station papa and long-term upper ocean study site. J. Geophys. Res, 95 (C9).

Gettelman, A., H. Morrison, and S.J. Ghan (2008). A new two-moment bulk stratiform cloud microphysics scheme in the Community Atmosphere Model, version 3 (CAM3). Part II: Single-column and global results. Journal of Climate 21(15): 3660-3679.

Griffies, S. (2004). Fundamentals of ocean climate models. Princeton University Press, 434pp.

Hersbach, H. and co-authors (2020). The ERA5 global reanalysis. Q. J. Roy.Met. Soc., 146, 730, 1999-2049, https://doi.org/10.1002/qj.3803.

Holland, M.M., D. A. Bailey, B. P. Briegleb, B. Light, and E. Hunke (2012). Improved sea ice shortwave radiation physics in CCSM4: the impact of melt ponds and aerosols on Arctic sea ice. J. Climate, 25(5): 1413–1430, 2012. doi:10.1175/ JCLI-D-11-00078.1.

Hunke, E. C., and Dukowicz, J. K. (1997). An elastic-viscous-plastic model for sea ice dynamics. Journal of Physical Oceanography, 27(9), 1849-1867.

Hunke, E. C., Lipscomb, W. H., & Turner, A. K. (2010). CICE: the Los Alamos Sea Ice Model Documentation and Software User's Manual Version 4.1 LA-CC-06-012. T-3 Fluid Dynamics Group, Los Alamos National Laboratory, 675.

Hurrell, James W., et al. (2013). The community earth system model: a framework for collaborative research. Bulletin of the American Meteorological Society 94(9):1339-1360.

Iacono M.J., J. S. Delamere, E. J. Mlawer, M. W. Shephard, S. A. Clough, and W. D. Collins (2008). Radiative forcing by long-lived greenhouse gases: Calculations with the AER radiative transfer models, J. Geophys. Res.: Atmospheres, 113(D13). doi:10.1029/2008JD009944.

IPCC (2013). Climate Change: The Physical Science Basis. Contribution of Working Group I to the Fifth Assessment Report of the Intergovernmental Panel on Climate Change [Stocker, T.F., D. Qin, G.-K. Plattner, M. Tignor, S.K. Allen, J. Boschung, A. Nauels, Y. Xia, V. Bex and P.M. Midgley (eds.)]. Cambridge University Press, Cambridge, United Kingdom and New York, NY, USA, 1535 pp, doi:10.1017/CBO9781107415324.

Kalnay, E., Kanamitsu, M., Kistler, R., Collins, W., Deaven, D., Gandin, L., ... & Zhu, Y. (1996). The NCEP/NCAR 40-year reanalysis project. Bulletin of the American Meteorological Society, 77(3), 437-471.

Lindvall, J., G. Svensson and R. Caballero (2017). The impact of changes in parameterizations of surface drag and vertical diffusion on the large-scale circulation in the Community Atmosphere Model (CAM5). *Clim Dyn*, **48,** 3741–3758 (2017). https://doi.org/10.1007/s00382-016-3299-9.

Liu X., R. C. Easter, S. J. Ghan, R. Zaveri, P. Rasch, X. Shi, J.-F. Lamarque, A. Gettelman, H. Morrison, F. Vitt, A. Conley, S. Park, R. Neale, C. Hannay, A. M. L. Ekman, P. Hess, N. Mahowald, W. Collins, M. J. Iacono, C. S. (2012). Toward a minimal representation of aerosols in climate models: description and evaluation in the Community Atmosphere Model CAM5. Geosci. Model Dev., 5(3):709–739. doi: 10.5194/gmd-5-709-2012.

Madec, G., and M. Imbard (1996). A global ocean mesh to overcome the north pole singularity. Clim. Dyn., 12, 381-388.

Madec, G. et al (2008). NEMO ocean engine. Institut Pierre Simon Laplace, Note du Pole de Modelisation 27, 2008. URL: http://www.nemo-ocean.eu/content/download/21612/97924/ file/NEMO_book_3_4.pdf.

McFarlane, N. A., 1987: The effect of orographically excited wave drag on the general circulation of the lower stratosphere and troposphere. J. Atmos. Sci., 44, 1775–1800.

Morrison, H. and A. Gettelman (2008). "A new two-moment bulk stratiform cloud microphysics scheme in the Community Atmosphere Model, version 3 (CAM3). Part I: Description and numerical tests." Journal of Climate 21, 15, 3642-3659.

Neale R.B. et al. (2010). Description of the NCAR Community Atmosphere Model (CAM 5.0). NCAR Technical Note NCAR/TN-4861STR, National Center for Atmospheric Research. http://www.cesm.ucar.edu/models/cesm1.1/cam/docs/description/cam5_desc.pdf.

Oleson, K. W., et al. (2013). Technical description of version 4.5 of the Community Land Model (CLM). NCAR Tech. Note NCAR/TN-503+ STR. National Center for Atmospheric Research, Boulder, CO, 422 pp. doi: 10.5065/D6RR1W7M.

Park. S. and C. S. Bretherton (2009). The University of Washington shallow convection and moist turbulence schemes and their impact on climate simulations with the Community Atmosphere Model. J. Climate, 22(12):3449–3469, 2009. doi:10.1175/2008JCLI2557.1.

Patera A.T. (1984). A spectral element method for fluid dynamics - Laminar flow in a channel expansion. Journal of Computational Physics, 54:468--488, 1984.

Pincus, R., H. W. Barker, and J.-J. Morcrette (2003). A fast, flexible, approximate technique for computing radiative transfer in inhomogeneous cloud fields. J. Geophys. Res.: Atmospheres, 108(D13), 2003. doi: 10.1029/2002JD003322.

Rancic, M., R. Purser, and F. Mesinger (1996). A global shallow-water model using an expanded spherical cube: Gnomonic versus conformal coordinates, Q. J. R. Meteorol. Soc., 122, 959–982.

Raymond, D. J., and A. M. Blyth (1986). A stochastic mixing model for non-precipitating cumulus clouds, *J. Atmos. Sci.*, *43*, 2708–2718.

Raymond, D. J., and A. M. Blyth (1992). Extension of the stochastic mixing model to cumulonimbus clouds, *J. Atmos. Sci.*, *49*, 1968–1983.

Richter, J. H., and P. J. Rasch (2008). Effects of convective momentum transport on the atmospheric circulation in the community atmosphere model, version 3, *J. Climate*, *21*, 1487–1499, 2008.

Richter, J. H., F. Sassi, and R. R. Garcia (2010). Toward a Physically Based Gravity Wave Source Parameterization in a General Circulation Model. *J. Atmos. Sci.*, **67**, 136–156, https://doi.org/10.1175/2009JAS3112.1.

Richter, J. H., A. Solomon and J.T. Bacmeister (2014). Effects of vertical resolution and nonorographic gravity wave drag on the simulated climate in the Community Atmosphere Model, version 5. Journal of Advances in Modeling Earth Systems, 6(2), 357-383.

Sanna, A., A. Borrelli, P. Athanasiadis, S. Materia, A. Storto, S. Tibaldi, S. Gualdi (2017). CMCC-SPS3: CMCC-SPS3: The CMCC Seasonal Prediction System 3. Centro Euro-Mediterraneo sui Cambiamenti Climatici. CMCC Tech. Rep. RP0285, 61pp. Available at adress: https://www.cmcc.it/it/publications/rp0285-cmcc-sps3-the-cmcc-seasonal-prediction-system-3

Sadourny, R. (1972): Conservative finite-difference approximations of the primitive equations on quasi uniform spherical grids, Mon. Wea. Rev., *100* (2), 136–144.

Simmons, A. J., and D. M. Burridge (1981): An energy and angular momentum conserving vertical finite-difference scheme and hybrid vertical coordinates, *Mon. Wea. Rev.*, *109*, 758–766.

Simmons, H. L., S. R. Jayne, L. C. St. Laurent, and A. J. Weaver (2004). Tidally driven mixing in a numerical model of the ocean general circulation. Ocean Modelling, 245–263.

Subin, Z. M., Riley, W. J., & Mironov, D. (2012). An improved lake model for climate simulations: Model structure, evaluation, and sensitivity analyses in CESM1. Journal of Advances in Modeling Earth Systems, 4(1).

Swenson, S. C., Lawrence, D. M., & Lee, H. (2012). Improved simulation of the terrestrial hydrological cycle in permafrost regions by the Community Land Model. Journal of Advances in Modeling Earth Systems, 4(3).

Zalesak, S. T. (1979). Fully multidimensional flux corrected transport algorithms for fluids. J. Comput. Phys., 31.

Zhang, J. L. and Rothrock, D. A. (2003). Modeling global sea ice with a thickness and enthalpy distribution model in generalized curvilinear coordinates, Mon. Weather Rev., 131, 845–861.

Zhang, G. J., and N. A. McFarlane (1995). Sensitivity of climate simulations to the parameterization of cumulus convection in the Canadian Climate Centre general circulation model, *Atmosphere-Ocean*, *33*, 407–446.